

# Tunable double optomechanically induced transparency in an optomechanical system

Peng-Cheng Ma<sup>1,2,3</sup>, Jian-Qi Zhang<sup>2,\*</sup>, Yin Xiao<sup>1</sup>, Mang Feng<sup>2,†</sup> and Zhi-Ming Zhang<sup>1‡</sup>

<sup>1</sup>*Laboratory of Nanophotonic Functional Materials and Devices (SIPSE),  
and Laboratory of Quantum Engineering and Quantum Materials,  
South China Normal University, Guangzhou 510006, China*

<sup>2</sup>*State Key Laboratory of Magnetic Resonance and Atomic and Molecular Physics,  
Wuhan Institute of Physics and Mathematics, Chinese Academy of Sciences, Wuhan 430071, China*

<sup>3</sup>*School of Physics and Electronic Electrical Engineering,  
Huaiyin Normal University, Huaian 223300, China*

We study the dynamics of a driven optomechanical cavity coupled to a charged nanomechanical resonator via Coulomb interaction, in which the tunable double optomechanically induced transparency (OMIT) can be observed from the output field at the probe frequency by controlling the strength of the Coulomb interaction. We calculate the splitting of the two transparency windows, which varies near linearly with the Coulomb coupling strength in a robust way against the cavity decay. Our double-OMIT is much different from the previously mentioned double-EIT or double-OMIT, and might be applied to measure the Coulomb coupling strength.

PACS numbers: 42.50.Wk, 46.80.+j, 41.20.Cv

## I. INTRODUCTION

Recently, significant theoretical and experimental efforts have been paid on studying the characteristic and application of nanomechanical resonators (NRs) [1–4]. NRs own some important properties, such as phonon induced transparency [5], phonon blockade [6], and high harmonic generation [7], and can be employed in many applications as, for example, single photon source [8], single phonon source [9], biological sensor [10], quantum information processing [11], and quantum metrology [12, 13].

In combination with an optical cavity, an NR turns to be an optomechanical system [14–17], in which the NR interacts with the cavity mode via the radiation pressure force and enables observation of the NR-induced quantum mechanical behaviors from the output light of the cavity. Until now, there have been a lot of theoretical predictions in such optomechanical systems, for example, photon blockade [18], Kerr effect [19], optomechanically induced transparency (OMIT) [20], quantum information transfer [21], normal-mode splitting [22], and some of them have been demonstrated experimentally, such as, OMIT [23–26], slow light [24], frequency transfer [27], and normal-mode splitting [28].

The present work is focused on the OMIT effect in the optomechanical cavity. The OMIT is a kind of induced transparency caused by the radiation pressure in an optomechanical system [20, 23], which stands at the center of current studies for optomechanics. We have noticed recent OMIT-relevant work on four-wave mixing [29], superluminal and ultraslow light propagation

[30, 31], quantum router [32], and precision measurement of electrical charge [33]. On the other hand, double electromagnetic induced transparency (EIT) [34–36] is a hot topic over recent years, which extends conventional EIT to the one with double transparency windows, and discovers some new physics and applications. This arises a question: what would happen in an OMIT with two transparency windows (i.e., double-OMIT)? To the best of our knowledge, there have been a few theoretical schemes [37–39] for the double-OMIT with different models, using a nonlinear crystal or a qubit in an optomechanical cavity [37, 38], and using a ring cavity with two movable mirrors [39]. However, in all the schemes mentioned above, the frequency of the transparency light for the double-EIT/OMIT cannot be changed due to the fixed coupling for splitting the transparency windows.

In this work, we demonstrate a tunable double-OMIT observable in an optomechanical system, in which the two NRs are charged and the two transparency windows are split due to the Coulomb interaction. Specifically, our optomechanical system consists of an optomechanical cavity and a NR outside, as sketched in Fig. 1, where the NR of the optomechanical cavity (i.e., NR<sub>1</sub>) not only couples to the cavity field by the radiation pressure, but also interacts with the NR outside the cavity (i.e., NR<sub>2</sub>) through the tunable Coulomb interaction, which can be controlled by the bias voltages on the NRs.

Compared with the conventional OMIT with a single transparency window [23–26], our scheme owns some favorable features: (i) The two output lights with different frequencies are controlled by a single driving light; (ii) Our scheme is robust to the cavity decay, and the transparency windows are with narrow profiles; (iii) We find that the two windows of the double-OMIT are apart near linearly with respect to the Coulomb coupling strength. The feature reminds us of a practical application of the double-OMIT for precisely detecting the Coulomb coupling strength. In this context, we have to emphasize

\*Electronic address: changjianqi@gmail.com

†Electronic address: mangfeng@wipm.ac.cn

‡Electronic address: zmzhang@scnu.edu.cn

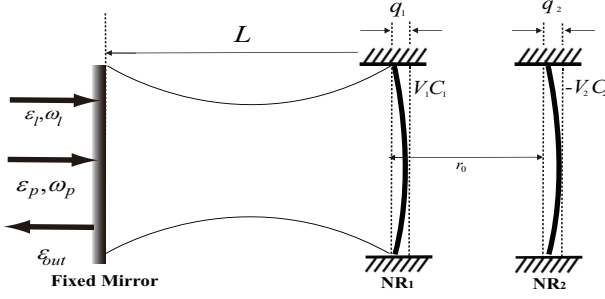


FIG. 1: Schematic diagram of the system. A high-quality Fabry-Pérot cavity consists of a fixed mirror and a movable mirror NR<sub>1</sub>. NR<sub>1</sub> is charged by the bias gate voltage  $V_1$  and subject to the Coulomb force due to another charged NR<sub>2</sub> with the bias gate voltage  $-V_2$ . The optomechanical cavity of the length  $L$  is driven by two light fields, one of which is the pump field  $\varepsilon_l$  with frequency  $\omega_l$  and the other of which is the probe field  $\varepsilon_p$  with frequency  $\omega_p$ . The output field is represented by  $\varepsilon_{out}$ .  $q_1$  and  $q_2$  represent the small displacements of NR<sub>1</sub> and NR<sub>2</sub> from their equilibrium positions, with  $r_0$  the equilibrium distance between the two NRs.

that our proposal is essentially different from the previous ideas [38, 39], where the double-OMIT is caused by the frequency difference between the two NRs and the frequencies of the transparency lights are fixed. In contrast, our studied double-OMIT can be observed even for two identical NRs, and the frequency of the transparency light can be selected by tuning the Coulomb coupling under a constant driving light.

This paper is structured as follows. In Sec. II we present the model and the analytical expressions of the optomechanical system and obtain the steady-state mean values. Sec. III includes numerical calculations for the double-OMIT based on recent experimental parameters. The feasibility of precision measurement of the Coulomb coupling strength between the two NRs is discussed in Sec. IV and we also justify the robustness of our approach against the cavity decay. The last section is a brief conclusion.

## II. THE MODEL AND THE SOLUTIONS

For the system in Fig. 1, the Hamiltonian is given by,

$$H_{whole} = \hbar\omega_c c^\dagger c + \left(\frac{p_1^2}{2m_1} + \frac{1}{2}m_1\omega_1^2 q_1^2\right) + \left(\frac{p_2^2}{2m_2} + \frac{1}{2}m_2\omega_2^2 q_2^2\right) - \hbar g c^\dagger c q_1 + H_C + i\hbar\varepsilon_l(c^\dagger e^{-i\omega_l t} - h.c.) + i\hbar(c^\dagger \varepsilon_p e^{-i\omega_p t} - h.c.), \quad (1)$$

where the first term is for the single-mode cavity field with frequency  $\omega_c$  and annihilation (creation) operator  $c$  ( $c^\dagger$ ). The second (third) term describes the vibration of the charged NR<sub>1</sub> (NR<sub>2</sub>) with frequency  $\omega_1$  ( $\omega_2$ ), effective mass  $m_1$  ( $m_2$ ), position  $q_1$  ( $q_2$ ) and momentum operator

$p_1$  ( $p_2$ ) [32]. NR<sub>1</sub> couples to the cavity field due to the radiation pressure with the coupling strength  $g = \frac{\omega_c}{L}$  with  $L$  being the cavity length.

The fifth term  $H_C$  in Eq.(1) presents the Coulomb coupling between the charged NR<sub>1</sub> and NR<sub>2</sub> [40], where the NR<sub>1</sub> and NR<sub>2</sub> take the charges  $C_1 V_1$  and  $-C_2 V_2$ , with  $C_1$  ( $C_2$ ) and  $V_1$  ( $-V_2$ ) being the capacitance and the voltage of the bias gate, respectively. So the Coulomb coupling between NR<sub>1</sub> and NR<sub>2</sub> is given by

$$H_C = \frac{-C_1 V_1 C_2 V_2}{4\pi\varepsilon_0 |r_0 + q_1 - q_2|},$$

where  $r_0$  is the equilibrium distance between NR<sub>1</sub> and NR<sub>2</sub>,  $q_1$  and  $q_2$  represent the small displacements of NR<sub>1</sub> and NR<sub>2</sub> from their equilibrium positions, respectively. In the case of  $r_0 \gg q_1, q_2$ , with the second order expansion, the Hamiltonian above is rewritten as

$$H_C = \frac{-C_1 V_1 C_2 V_2}{4\pi\varepsilon_0 r_0} \left[1 - \frac{q_1 - q_2}{r_0} + \left(\frac{q_1 - q_2}{r_0}\right)^2\right],$$

where the linear term may be absorbed into the definition of the equilibrium positions, and the quadratic term includes a renormalization of the oscillation frequency for both NR<sub>1</sub> and NR<sub>2</sub>. This implies a reduced form

$$H_C = \hbar\lambda q_1 q_2,$$

where  $\lambda = \frac{C_1 V_1 C_2 V_2}{2\pi\hbar\varepsilon_0 r_0^3}$  [40–42].

The last two terms in Eq. (1) describe the interactions between the cavity field and the two input fields, respectively. The strong (weak) pump (probe) field owns the frequency  $\omega_l$  ( $\omega_p$ ) and the amplitude  $\varepsilon_l = \sqrt{2\kappa\wp_l/\hbar\omega_l}$  ( $\varepsilon_p = \sqrt{2\kappa\wp_p/\hbar\omega_p}$ ), where  $\wp_l$  ( $\wp_p$ ) is the power of the pump (probe) field and  $\kappa$  is the cavity decay rate.

In a frame rotating with the frequency  $\omega_l$  of the pump field, the Hamiltonian of the total system Eq.(1) can be rewritten as,

$$H = \hbar\Delta_c c^\dagger c + \left(\frac{p_1^2}{2m_1} + \frac{1}{2}m_1\omega_1^2 q_1^2\right) + \left(\frac{p_2^2}{2m_2} + \frac{1}{2}m_2\omega_2^2 q_2^2\right) - \hbar g c^\dagger c q_1 + \hbar\lambda q_1 q_2 + i\hbar\varepsilon_l(c^\dagger - c) + i\hbar(c^\dagger \varepsilon_p e^{-i\delta t} - h.c.), \quad (2)$$

where  $\Delta_c = \omega_c - \omega_l$  is the detuning of the pump field from the bare cavity, and  $\delta = \omega_p - \omega_l$  is the detuning of the probe field from the pump field.

Considering photon losses from the cavity and the Brownian noise from the environment, we may describe the dynamics of the system governed by Eq. (2) using following nonlinear quantum Langevin equations [32],

$$\begin{aligned} \dot{q}_1 &= \frac{p_1}{m_1}, \\ \dot{p}_1 &= -m_1\omega_1^2 q_1 - \hbar\lambda q_2 + \hbar g c^\dagger c - \gamma_1 p_1 + \sqrt{2\gamma_1}\xi_1(t), \\ \dot{q}_2 &= \frac{p_2}{m_2}, \\ \dot{p}_2 &= -m_2\omega_2^2 q_2 - \hbar\lambda q_1 - \gamma_2 p_2 + \sqrt{2\gamma_2}\xi_2(t), \\ \dot{c} &= -[\kappa + i(\Delta_c - gq_1)]c + \varepsilon_l + \varepsilon_p e^{-i\delta t} + \sqrt{2\kappa}c_{in}, \quad (3) \end{aligned}$$

where  $\gamma_1$  and  $\gamma_2$  are the decay rates for NR<sub>1</sub> and NR<sub>2</sub>, respectively. The quantum Brownian noise  $\xi_1$  ( $\xi_2$ ) comes from the coupling between NR<sub>1</sub> (NR<sub>2</sub>) and its own environment with zero mean value [43].  $c_{in}$  is the input vacuum noise operator with zero mean value [43]. Under the mean field approximation  $\langle Qc \rangle = \langle Q \rangle \langle c \rangle$  [20], the mean value equations are given by

$$\begin{aligned}\langle \dot{q}_1 \rangle &= \frac{\langle p_1 \rangle}{m_1}, \\ \langle \dot{p}_1 \rangle &= -m_1 \omega_1^2 \langle q_1 \rangle - \hbar \lambda \langle q_2 \rangle + \hbar g \langle c^\dagger \rangle \langle c \rangle - \gamma_1 \langle p_1 \rangle, \\ \langle \dot{q}_2 \rangle &= \frac{\langle p_2 \rangle}{m_2}, \\ \langle \dot{p}_2 \rangle &= -m_2 \omega_2^2 \langle q_2 \rangle - \hbar \lambda \langle q_1 \rangle - \gamma_2 \langle p_2 \rangle, \\ \langle \dot{c} \rangle &= -[\kappa + i(\Delta_c - g \langle q_1 \rangle)] \langle c \rangle + \varepsilon_l + \varepsilon_p e^{-i\delta t},\end{aligned}\quad (4)$$

which is a set of nonlinear equations and the steady-state response in the frequency domain is composed of many frequency components. We suppose the solution with the following form [33]

$$\begin{aligned}\langle q_1 \rangle &= q_{1s} + q_{1+} \varepsilon_p e^{-i\delta t} + q_{1-} \varepsilon_p^* e^{i\delta t}, \\ \langle p_1 \rangle &= p_{1s} + p_{1+} \varepsilon_p e^{-i\delta t} + p_{1-} \varepsilon_p^* e^{i\delta t}, \\ \langle q_2 \rangle &= q_{2s} + q_{2+} \varepsilon_p e^{-i\delta t} + q_{2-} \varepsilon_p^* e^{i\delta t}, \\ \langle p_2 \rangle &= p_{2s} + p_{2+} \varepsilon_p e^{-i\delta t} + p_{2-} \varepsilon_p^* e^{i\delta t}, \\ \langle c \rangle &= c_s + c_+ \varepsilon_p e^{-i\delta t} + c_- \varepsilon_p^* e^{i\delta t},\end{aligned}\quad (5)$$

where each quantity contains three items  $O_s$ ,  $O_+$ ,  $O_-$  (with  $O \in \{q_1, p_1, q_2, p_2, c\}$ ), corresponding to the responses at the frequencies  $\omega_l$ ,  $\omega_p$ , and  $2\omega_l - \omega_p$ , respectively [44]. In the case of  $O_s \gg O_\pm$ , Eq. (4) can be solved by treating  $O_\pm$  as perturbations. After substituting Eq. (5) into Eq. (4), and ignoring the second-order terms, we obtain the steady-state mean values of the system as

$$\begin{aligned}p_{1s} &= p_{2s} = 0, \\ q_{1s} &= \frac{\hbar g |c_s|^2}{m_1 \omega_1^2 - \frac{\hbar^2 \lambda^2}{m_2 \omega_2^2}}, \\ q_{2s} &= \frac{\hbar \lambda q_{1s}}{-m_2 \omega_2^2}, \\ c_s &= \frac{\varepsilon_l}{i\Delta + \kappa}, \\ |c_s|^2 &= \frac{|\varepsilon_l|^2}{\Delta^2 + \kappa^2},\end{aligned}\quad (6)$$

with  $\Delta = \Delta_c - g q_{1s}$ , and

$$c_+ = \frac{[\kappa - i(\Delta + \delta)][(\delta^2 - \omega_1^2 + i\delta\gamma_1) - G] - 2i\omega_1\beta}{[\Delta^2 - (\delta + i\kappa)^2][(\delta^2 - \omega_1^2 + i\delta\gamma_1) - G] + 4\Delta\omega_1\beta}, \quad (7)$$

where  $\beta = \frac{|c_s|^2 \hbar g^2}{2m\omega_1}$  and  $G = \frac{\hbar^2 \lambda^2}{m_1 m_2 (\delta^2 - \omega_2^2 + i\delta\gamma_2)}$ . When there is no Coulomb coupling  $\lambda$  (i.e.,  $G = 0$ ) between the two NRs, Eq. (7) is reduced to Eq. (5) in Ref. [20]. However, different from the output field in Ref. [20] involving a single center frequency for the single-mode

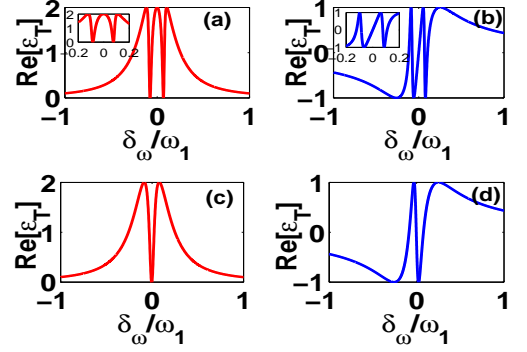


FIG. 2: (Color online) (a) The absorption  $Re[\varepsilon_T]$  and (b) the dispersion  $Im[\varepsilon_T]$  as functions of  $\delta_\omega/\omega_1$  under the Coulomb interaction. (c) The absorption  $Re[\varepsilon_T]$  and (d) the dispersion  $Im[\varepsilon_T]$  as functions of  $\delta_\omega/\omega_1$  in the absence of the Coulomb interaction.  $\delta_\omega = \delta - \omega_1$  is the detuning from the central line of the sideband,  $\lambda_l = 1064$  nm,  $L = 25$  mm,  $\omega_1 = \omega_2 = 2\pi \times 947 \times 10^3$  Hz, the quality factor  $Q_1 = \frac{\omega_1}{\gamma_1} (= Q_2 = \frac{\omega_2}{\gamma_2}) = 6700$ ,  $m_1 = m_2 = 145$  ng,  $\kappa = 2\pi \times 215 \times 10^3$  Hz,  $\wp_l = 2$  mW, and  $\lambda = 8 \times 10^{35}$  Hz/m<sup>2</sup> [27].

OMIT, there are two centers with different frequencies in our scheme due to the Coulomb interaction. As a result, under the actions of the radiation pressure and the probe light, two OMITs with different centers are reconstructed, yielding the double-OMIT.

Making use of the input-output relation of the cavity [45]

$$\varepsilon_{out}(t) + \varepsilon_p e^{-i\delta t} + \varepsilon_l = 2\kappa \langle c \rangle,$$

and

$$\varepsilon_{out}(t) = \varepsilon_{outs} + \varepsilon_{out+} \varepsilon_p e^{-i\delta t} + \varepsilon_{out-} \varepsilon_p^* e^{i\delta t},$$

we obtain

$$\varepsilon_{out+} = 2\kappa c_+ - 1,$$

which can be measured by homodyne technique [45]. This output light  $\varepsilon_{out+}$  is of the same frequency  $\omega_p$  as the probe field. Defining

$$\varepsilon_T = \varepsilon_{out+} + 1 = 2\kappa c_+, \quad (8)$$

yields the real and imaginary parts, with  $Re[\varepsilon_T]$  and  $Im[\varepsilon_T]$ , representing the absorption and dispersion of the optomechanical system, respectively [20].

### III. DOUBLE-OMIT IN THE OUTPUT FIELD

We present below the feasibility of the tunable double-OMIT in the optomechanical system, and the relationship between the double-OMIT and the Coulomb interaction between the two NRs. As an estimate for Eq.(8), we employ the parameters from the recent experiment

[27] in the observation of the normal-mode splitting. For simplicity, we first consider two identical NRs in our numerics, which is not essentially different in physics from the case of two different NRs. We will also treat the different NRs later.

As shown in Fig. 2, the absorption  $Re[\varepsilon_T]$  and dispersion  $Im[\varepsilon_T]$  of the output field are plotted as functions of  $\delta_\omega/\omega_1 = (\delta - \omega_1)/\omega_1$  for different Coulomb couplings. We may find that the output lights for the probe field behave from the double-OMIT to the single-mode OMIT with diminishing Coulomb coupling. The physics behind the double-OMIT phenomenon can be understood from the interference [23, 46] and the level configuration in Fig. 3.

The OMIT originates from the radiation pressure coupling an optical mode to a mechanical mode. The simultaneous presence of the pump and probe fields generates a radiation-pressure force oscillating at the frequency difference  $\delta = \omega_p - \omega_l$ . If this frequency difference is close to the resonance frequency  $\omega_1$  of NR<sub>1</sub>, the mechanical mode starts to oscillate coherently. This in turn gives rise to the Stokes- and anti-Stokes scattering of light from the strong pump field. If the system is operated within the resolved-sideband regime  $\kappa \ll \omega_1$ , the Stokes scattering is strongly suppressed since it is highly off-resonant with the optical cavity. We can therefore assume that only an anti-Stokes field with frequency  $\omega_p = \omega_l + \omega_1$  builds up inside the cavity. However, since this field is degenerate with the probe field sent into the cavity, the two fields interfere destructively, suppressing the case of a single transparency window for the output beam. Thus the OMIT occurs. As it depends on quantum interference, the OMIT is sensitive to phase disturbances. The coupling between NR<sub>1</sub> and NR<sub>2</sub> not only adds a fourth level, as shown in Fig. 3, but also breaks down the symmetry of the OMIT interference, and thereby produces a spectrally sharp bright resonance within the OMIT line shape. Then the single OMIT transparency window is split into two transparency windows, which yields the double-OMIT.

#### IV. MEASUREMENT OF THE COUPLING STRENGTH BETWEEN NR<sub>1</sub> AND NR<sub>2</sub>

To further explore the characteristic of the tunable double-OMIT, we plot the absorption  $Re[\varepsilon_T]$  as functions of  $\delta_\omega/\omega_1$  and  $\lambda$ . One can find from Fig. 4 that only a single transparency window appears at  $\delta_\omega = 0$  ( $\delta = \omega_1$ ) in the absence of the Coulomb coupling, and the single transparency window is split into two transparency windows once the Coulomb coupling is present. The two transparency windows are more and more apart with the increase of  $\lambda$ . The two minima of the absorption in Fig. 4 can be evaluated by

$$\left. \frac{dRe[\varepsilon_T]}{d\delta_\omega} \right|_{\delta_\omega=\delta_{\omega+}} = 0, \quad \left. \frac{dRe[\varepsilon_T]}{d\delta_\omega} \right|_{\delta_\omega=\delta_{\omega-}} = 0, \quad (9)$$

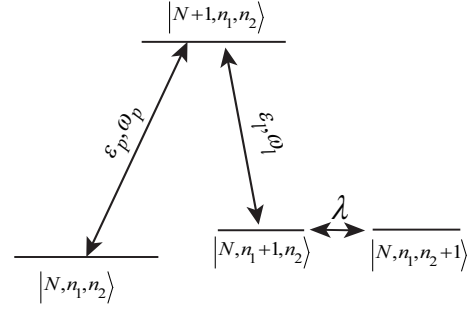


FIG. 3: Schematic of the energy-level diagram in the cavity optomechanical system, where  $|N\rangle$ ,  $|n_1\rangle$  and  $|n_2\rangle$  denote the number states of the cavity photon, and NR<sub>1</sub> and NR<sub>2</sub> phonons, respectively.  $|N, n_1, n_2\rangle \longleftrightarrow |N+1, n_1, n_2\rangle$  transition changes the cavity field,  $|N+1, n_1, n_2\rangle \longleftrightarrow |N, n_1+1, n_2\rangle$  transition is caused by the radiation pressure coupling, and  $|N, n_1+1, n_2\rangle \longleftrightarrow |N, n_1, n_2+1\rangle$  transition is induced by the Coulomb coupling [23, 46].

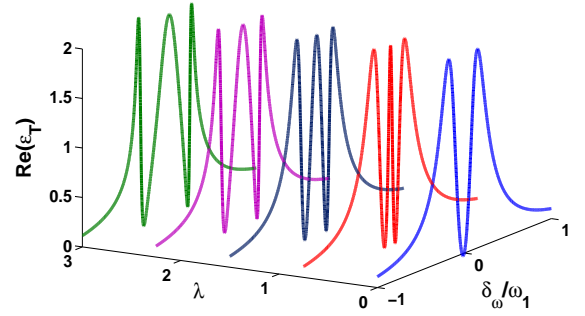


FIG. 4: (Color online) The absorption  $Re[\varepsilon_T]$  as functions of  $\delta_\omega/\omega_1$  and  $\lambda$  (units of  $\lambda_0 = 8 \times 10^{35}$  Hz/m<sup>2</sup>). Other parameters take the same values as in Fig. 2.

where the detunings  $\delta_{\omega+}$  and  $\delta_{\omega-}$  are the points with absorption minima. So the separation of the minima is  $d = |\delta_{\omega+} - \delta_{\omega-}|$ , as plotted in Fig. 5, where the almost linear increase of  $d$  with  $\lambda$  within the regime  $\lambda = \{0, 15\lambda_0\}$  reminds us of the possibility to detect the Coulomb coupling strength between NR<sub>1</sub> and NR<sub>2</sub> by measuring the separation  $d$  in the absorption spectrum  $Re[\varepsilon_T]$  of the output field. From Fig. 5, one can calculate the measuring sensitivity by  $\frac{\partial d}{\partial \lambda}$  on the order of  $10^{-31}$  m<sup>2</sup>. Considering a Coulomb coupling change  $\Delta F$  due to a slight deviation  $q_1$ , we have  $\Delta F = \hbar \lambda q_1$ . Provided  $q_1 \approx 0.1$  nm, we may assess  $\partial \Delta F / \partial d$  to be of the order of  $10^{-13}$  N/Hz, implying the possible precision of measuring  $\Delta F$  decided by the resolution of  $d$  in the absorption spectrum.

Fig. 6 presents the variation of the absorption  $Re(\varepsilon_T)$  with respect to  $\delta_\omega/\omega_1$  for different cavity decay rates, where the maxima (i.e., the points A, B and C) and the minima (i.e., the points D and E) of the curves remain unchanged in the parameter changes, but the profiles of the transparency window become narrower and sharper with the cavity decay rate  $\kappa$  increasing. Provided a fixed

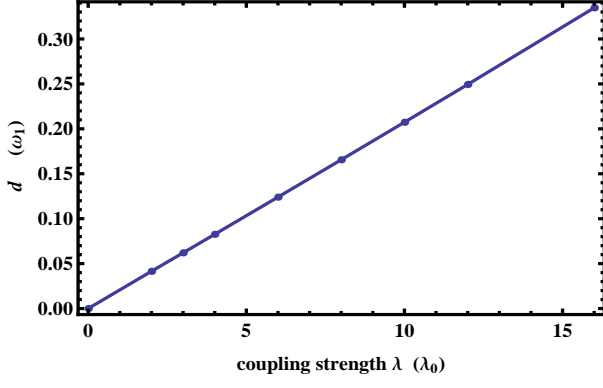


FIG. 5: The separation  $d$  (units of  $\omega_1$ ) between the two minima in the absorption spectrum as a function of the coupling strength  $\lambda$  (units of  $\lambda_0 = 8 \times 10^{35} \text{ Hz/m}^2$ ). Other parameters take the same values as in Fig. 2.

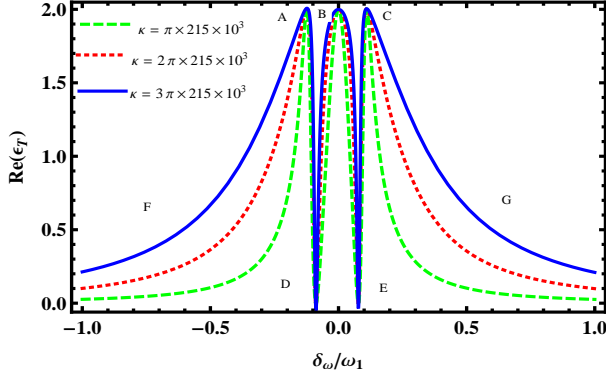


FIG. 6: (Color online) The absorption  $Re[\epsilon_T]$  as a function of  $\delta\omega/\omega_1$  with different cavity decay rates,  $\kappa = \pi \times 215 \times 10^3 \text{ Hz}$  (green dashed line),  $\kappa = 2\pi \times 215 \times 10^3 \text{ Hz}$  (red dotted line),  $\kappa = 3\pi \times 215 \times 10^3 \text{ Hz}$  (blue solid line). Other parameters take the same values as in Fig. 2.

driving light, the bigger cavity decay will disturb the radiation pressure and makes it less precise in detecting the strength of the radiation pressure, which is reflected in Fig. 6 that the parts of the spectrum, FAD and ECG, become wider and wider with  $\kappa$  increasing. In contrast, the other parts of the spectrum, ADB and BEC, turn to be narrower and narrower, implying more precision in detecting the Coulomb interaction. In comparison with the previous proposals [12, 13] for detecting coupling strength, our double-OMIT can provide a more effective and suitable method to achieve a precision measurement due to the robustness against  $\kappa$  and the narrower profiles in the output light fields.

The robustness of our scheme can be understood as follows. When the Coulomb interaction and the driving light are fixed, the equilibrium position is decided by the strain of the NR. With the increase of the cavity decay rate, the radiation pressure in the optomechanical system decreases, while the NR will acquire a larger displacement to provide a larger strain for compensating the reduced

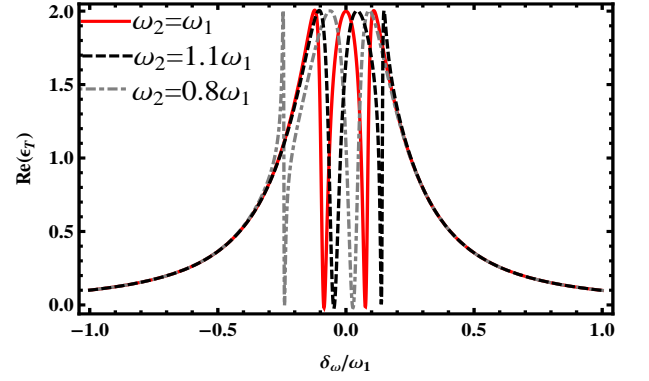


FIG. 7: (Color online) The absorption  $Re[\epsilon_T]$  as a function of  $\delta\omega/\omega_1$  for identical and different NR frequencies. Other parameters take the same values as in Fig. 2.

radiation pressure. The spectrum of the output becomes narrower for the larger displacement of the NR. In this way, our scheme can be robust against the cavity decay rate.

Moreover, for two different NRs, the results will be slightly different from those above for identical NRs. Considering  $\omega_1 \neq \omega_2$  in the calculation, we have plotted in Fig. 7 the absorption of the double-OMIT with larger separations of the minima in comparison with the identical NR case. It implies a more sensitivity to the coupling strength  $\lambda$  in the case of two different NRs. With respect to the  $\omega_1 = \omega_2$  case, the absorption curves move rightward (leftward) in the case of  $\omega_1 > \omega_2$  ( $\omega_1 < \omega_2$ ). The enhancement of the sensitivity to the Coulomb force can be calculated by Eq. (9) and  $d = |\delta\omega_+ - \delta\omega_-|$ , and is exemplified in Fig. 7 as 1.139 (1.529) times using  $\omega_2 = 1.1\omega_1$  ( $\omega_2 = 0.8\omega_1$ ).

We have to mention that the robustness discussed above is limited within the resolved regime ( $\kappa < \omega_1$ ) where the double-OMIT works. In contrast, the unresolved regime ( $\kappa > \omega_1$ ) blurs the sideband transitions, which makes the quantum interference unavailable.

## V. CONCLUSION

In conclusion, we have demonstrated the feasibility of the tunable double-OMIT in the optomechanical system under the Coulomb interaction between two charged NRs. To our knowledge, this is the first proposal for the tunable double-OMIT in the optomechanical system. Although our proposal is in principle extendable to other interactions, such as the dipole-dipole coupling, the Coulomb coupling, as a long-range interaction, is easier to control, and thereby more practical. We have to emphasize that our double-OMIT is neither a simple extension of the conventional OMIT nor a simple transformation of the previously discussed double-EIT. Due to narrow profiles of the transparency windows and robustness against dissipation, the double OMIT might be employed

for precisely detecting the Coulomb coupling strength. Therefore, we argue that our scheme have paved a new avenue towards the study of the OMIT with more transparency windows as well as the relevant application.

## ACKNOWLEDGMENTS

PCM thanks Lei-Lei Yan and Wan-Lu Song for their helps in the numerical simulation. JQZ thanks Yong Li for the helpful discussion. This work was supported

by the "973" Program (Grant No. 2011CBA00200, No. 2012CB922102 and No. 2013CB921804), the Major Research Plan of the NSFC (Grant No. 91121023), the NSFC (Grants No. 61378012, No. 60978009, No. 11274352 and No. 11304366), the SRFDPHEC (Grant No.20124407110009), the PCSIRT (Grant No. IRT1243), China Postdoctoral Science Foundation (Grant No. 2013M531771 and No. 2014T70760), Natural Science Funding for Colleges and Universities in Jiangsu Province (Grant No. 12KJD140002), and Program for Excellent Talents of Huaiyin Normal University(No. 11HSQNZ07).

- 
- [1] K. C. Schwab and M. L. Roukes, *Phys. Today* **58**, 36 (2005).
  - [2] X. Zhou, F. Hocke, A. Schliesser, A. Marx, H. Huebl, R. Gross, and T. J. Kippenberg, *Nat. Phys.* **9**, 179 (2013).
  - [3] P. C. Ma, Y. Xiao, Y. F. Yu, and Z. M. Zhang, *Opt. Express* **22**, 3621 (2014).
  - [4] J. Q. Zhang, S. Zhang, J. H. Zou, L. Chen, W. Yang, Y. Li, and M. Feng, *Opt. Express* **21**, 29695 (2013).
  - [5] H. Okamoto, A. Gourgout, C. Y. Chang, K. Onomitsu, I. Mahboob, E. Y. Chang, and H. Yamaguchi, *Nat. Phys.* **9**, 480 (2013).
  - [6] Y. X. Liu, A. Miranowicz, Y. B. Gao, J. Bajer, C. P. Sun, and F. Nori, *Phys. Rev. A* **82**, 032101 (2010).
  - [7] H. Xiong, L. G. Si, X. Y. Lü, X. X. Yang, and Y. Wu, *Opt. Lett.* **38**, 353 (2013).
  - [8] L. Qiu, L. Gan, W. Ding, and Z. Y. Li, *J. Opt. Soc. Am. B* **30**, 1683 (2013).
  - [9] K. V. Keesidis, S. D. Bennett, S. Portolan, M. D. Lukin, and P. Rabl, *Phys. Rev. B* **88**, 064105 (2013).
  - [10] K. Eom, H. S. Park, D. S. Yoon, and T. Kwon, *Phys. Rep.* **503**, 115 (2011).
  - [11] P. Rabl, S. J. Kolkowitz, F. H. L. Koppens, J. G. E. Harris, P. Zoller, and M. D. Lukin, *Nat. Phys.* **6**, 602 (2010).
  - [12] W. He, J. J. Li and K. D. Zhu, *Opt. Lett.* **35**, 339 (2010).
  - [13] J. J. Li and K. D. Zhu, *Appl. Phys. Lett.* **94**, 063116 (2009).
  - [14] T. J. Kippenberg and K. J. Vahala, *Opt. Express* **15**, 17172 (2007).
  - [15] T. J. Kippenberg and K. J. Vahala, *Science* **321**, 1172 (2008).
  - [16] F. Marquardt and S. M. Girvin, *Physics* **2**, 40 (2009).
  - [17] M. Aspelmeyer, P. Meystre, and K. Schwab, *Phys. Today* **65**, 29 (2012).
  - [18] P. Rabl *Phys. Rev. Lett.* **107**, 063601 (2011).
  - [19] Z. R. Gong, H. Ian, Y. X. Liu, C. P. Sun, and F. Nori, *Phys. Rev. A* **80**, 065801 (2009).
  - [20] G. S. Agarwal and S. Huang, *Phys. Rev. A* **81**, 041803 (2010).
  - [21] C. H. Dong, V. Fiore, M. C. Kuzyk, and H. L. Wang, *Science* **338**, 1609 (2012).
  - [22] J. M. Dobrindt, I. Wilson-Rae, and T. J. Kippenberg, *Phys. Rev. Lett.* **101**, 263602 (2008).
  - [23] S. Weis, R. Rivière, S. Deléglise, E. Gavartin, O. Arcizet, A. Schliesser, and T. J. Kippenberg, *Science* **330**, 1520 (2010).
  - [24] A. H. Safavi-Naeini, T. P. M. Alegre, J. Chan, M. Eichenfield, M. Winger, Q. Lin, J. T. Hill, D. Chang, and O. Painter, *Nature (London)* **472**, 69 (2011).
  - [25] M. Karuza, C. Biancofiore, M. Bawaj, C. Molinelli, M. Galassi, R. Natali, P. Tombesi, G. Di Giuseppe, and D. Vitali, *Phys. Rev. A* **88**, 013804 (2013).
  - [26] H. Xiong, L. G. Si, A. S. Zheng, X. Yang and Y. Wu, *Phys. Rev. A* **86**, 013815 (2012).
  - [27] J. T. Hill, A. H. Safavi-Naeini, J. Chan, and O. Painter, *Nat. Commun.* **3**, 1196 (2012).
  - [28] S. K. Gröblacher Hammerer, M. R. Vanner, and M. Aspelmeyer, *Nature (London)* **460**, 724 (2009).
  - [29] S. Huang and G. S. Agarwal, *Phys. Rev. A* **81**, 033830 (2010).
  - [30] J. D. Teufel, D. Li, M. S. Allman, K. Cicak, A. J. Sirois, J. D. Whittaker, and R. W. Simmonds, *Nature (London)* **471**, 204 (2011).
  - [31] D. Tarhan, S. Huang, and Ö. E. Müstecaplıoğlu, *Phys. Rev. A* **87** 013824 (2013).
  - [32] G. S. Agarwal and S. Huang, *Phys. Rev. A* **85**, 021801(R) (2012).
  - [33] J. Q. Zhang, Y. Li, M. Feng, and Y. Xu, *Phys. Rev. A* **86** 053806 (2012).
  - [34] Z. B. Wang, K. P. Marzlin, and B. C. Sanders, *Phys. Rev. Lett.* **97**, 063901 (2006).
  - [35] B. W. Shiao, M. C. Wu, C. C. Lin, and Y. C. Chen, *Phys. Rev. Lett.* **106**, 193006 (2011).
  - [36] S. J. Li, X. D. Yang, X. M. Cao, C. H. Zhang, C. D. Xie, and H. Wang, *Phys. Rev. Lett.* **101**, 073602 (2008).
  - [37] S. Shahidani, M. H. Naderi, and M. Soltanolkotabi, *Phys. Rev. A* **88**, 053813 (2013).
  - [38] H. Wang, X. Gu, Y. X. Liu, A. Miranowicz and F. Nori, *arXiv:1402.2764v1* (2014).
  - [39] S. Huang, *J. Phys. B: At. Mol. Opt. Phys.* **47**, 055504 (2014).
  - [40] W. K. Hensinger, D. W. Utami, H. S. Goan, K. Schwab, C. Monroe, and G. J. Milburn, *Phys. Rev. A* **72**, 041405(R) (2005).
  - [41] C. N. Ren, J. Q. Zhang, L. B. Chen and Y. J. Gu, *arXiv:1402.6434* (2014).
  - [42] L. Tian and P. Zoller, *Phys. Rev. Lett.* **93**, 266403 (2004).
  - [43] C. Genes, D. Vitali, P. Tombesi, S. Gigan, and M. Aspelmeyer, *Phys. Rev. A* **77**, 033804 (2008).
  - [44] S. Huang and G. S. Agarwal, *Phys. Rev. A* **83**, 023823 (2011).
  - [45] D. F. Walls and G. J. Milburn, *Quantum Optics* (Springer-Verlag, Berlin) (1994).
  - [46] J. A. Sedlacek, A. Schwettmann, H. Kübler, R. Löw, T.

Pfau, and J. P. Shaffer, *Nature Phys.* **8** 819 (2012).